Presented at the 29th European PV Solar Energy Conference and Exhibition, 22-26 September 2014, Amsterdam, The Netherlands

FAILURE MECHANISMS FOR SOLAR CELLS WITH LASER DOPED SELECTIVE EMITTER AND PLATED NI-CU METAL CONTACTS

W. Hördt, S.Kluska, C. Geisler, S. Hopman, J. Bartsch, A. Mondon, M. Glatthaar
Fraunhofer Institute for Solar Energy Systems ISE, Heidenhofstrasse 2, 79110 Freiburg, Germany,
Phone +49 761/4588-5019, wilhelm.hoerdt@ise.fraunhofer.de

ABSTRACT: Al-BSF solar cells with a laser doped selective emitter and plated Ni-Cu contacts are an attractive approach for industrial fabrication. Yet the contact adhesion of the plated Ni-Cu contacts due to diffusion barriers in the contact area and electrical stability against tempering induced non-ohmic Ni shunts are two main challenges for this cell concept. This work presents failure mechanisms of laser doped solar cells. Microscopic characterization analyzes process induced defects separately, which result in poor contact adhesion and non-ohmic shunting. A process route is presented, which yields in solar cells with pseudo fill factors above 80 % and a sufficient contact adhesion of 1 N/mm.
Keywords: Selective Emitter, Laser Doping, Laser Chemical Processing, Plated Contacts, Ni-Cu, Peel test

1 INTRODUCTION

Solar cell concepts with selective emitter design and plated contacts have been commercialized by BP Solar with the concept of a laser grooved buried contact solar cell [1] and by SUNTECH with the PLUTO technology [2]. Using the combination of laser doping and plated Ni-Cu contacts both cell concepts demonstrated high cell efficiencies of 18.3 % for BP Solar [3] and 20.3 % for SUNTECH [4]. RENA reached an solar cell efficiency of 18.6 % on an Al-BSF solar cell with Laser Chemical Processing [5]. For the fabrication of selective emitter design in combination with Ni-Cu plating one of the challenges limiting the success of these solar cell designs is the adhesion of the plated Ni-Cu contacts. An annealing step is favorable in order to form nickel silicides at the contact interface and improve the metal contact adhesion [6]. However, the annealing process can lead to the formation of nickel silicides (Ni_xSi_y) deep enough to penetrate the space charge region of the pn junction, which results in significant power losses of the solar cell [7, 8]. The optimization of the back-end processing chain (laser doping → plating → silicidation → soldering) of a solar cell with Ni-Cu contacts is important for their electrical performance and a suitable adhesion of the plated contacts. This work will analyze failure mechanisms for laser doped solar cells with plated contacts and show methods to prevent those failure mechanisms

2 EXPERIMENTAL SETUP

2.1 Cell Fabrication

In this work solar cells were fabricated using 156x156 mm² pseudo square p-type Cz Si wafers with a base resistivity of 1-3 Ωcm and random pyramids texture. The cell design was carried out into four 5x5 cm^2 cells per wafer with a 1.5 mm bus bar and 1.3 mm finger pitch on each cell. The full faced n-type emitter was produced by $POCl_3$ diffusion in a tube furnace resulting in 120 Ω resistivity. The front side passivation was done by PECVD SiN_x deposition and the back side contact by screen printed and fired Al. In addition a highly laser doped selective emitter (SE) was included into the process chain.

One approach for the SE laser doping was introduced in [9]. A green continuous wave (cw) laser (λ = 532 nm, P = 15 W) was guided onto the Si wafer surface by a galvanometric scanner head (SCANLAB-IntelliScan) with a scanning speed of v_{sc} = 5 m/s. A phosphorous wet film, which was spun directly onto the passivated Si surface after furnace diffusion provided the dopant source. This results in an average doping depth of 4.2 µm with sheet resistance of 9.6 Ω and a surface concentration of $5x10^{19}$ cm^{-3}. Another technology to create a SE is Laser Chemical Processing (LCP) which was presented by [10]. Here a green nanosecond pulsed laser with pulse duration of 40 ns and a linear axis moving the sample with a velocity of 100 mm/s was used. This results in an average doping depth of 1.2 µm with a sheet resistance of 6 Ω and a surface concentration of $1x10^{21}$ cm^{-3}. The laser doped fingers were set to a width of 150 µm and consisted of overlapping lines.

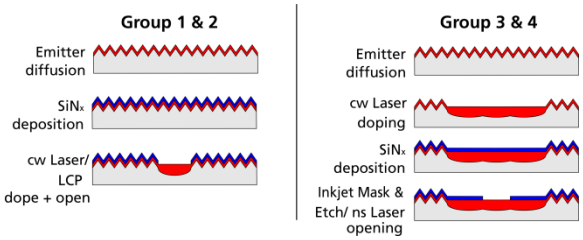

Figure 1: Process variation. Simultaneous laser doping and SiN_x opening in Group 1 with cw laser and LCP in Group 2. On the right side the doping and SiNx opening are split: cw laser doping → SiN_x → opening (Group 3 by Inkjet Mask & Etch, Group 4 by nanosecond laser ablation)

In this experiment four groups were produced with each group consisting of 20 solar cells. Figure 1 illustrates the process variations and these group arrangements. In group 1 and 2 the passivation layer was opened and the Si underneath was doped in one process step. The solar cells in group one featured the local SE doping by cw laser and phosphorous wet film and group 2 by LCP. In order to cover up the shallow doped regions at the edge of the laser doped lines in group 1 two extra groups were fabricated. Therefore, the laser doping of the Si wafer and SiN_x opening were fabricated in individual process steps. Two technologies for SiN_x structuring were used. In Group 3 the SiN_x layer was removed by buffered hydrogen fluoride (BHF). The opening layout was preset by an inkjet printed mask (Inkjet Mask & Etch), which allows a contact opening of about 30 µm.

Group 4 was structured with a green nanosecond pulsed laser with a pulse duration of 80 ns, which resulted in a contact opening of about 14 µm.

The front side metallization was deposited by Light Induced Ni Plating (LIP) with a RENA inline tool. All solar cells received a HF (1 %, 30s) pretreatment before plating. In order to analyze the influence of remaining surface diffusion barrier layers an extension of group 1 with a different pretreatment (10:1 BHF, 60 s) is presented here and is discussed in detail in [11]. The results will be denoted as "group 1-HF" and "group 1 - BHF". A harsh annealing step of 450 °C for 10 min at a forming gas atmosphere was performed in order to induce Ni_xSi_y formation. The full metal contact stack of Ni, Cu and Ag was plated after unreacted Ni was selectively removed in Piranha etchant after anneal.

2.2 Characterization

The electrical annealing stability was analyzed by measuring the pseudo light IV curve with a Sinton SunsV_{oc} tester. Here the pseudo fill factor (*pFF*) was measured before and after plating and annealing. Reverse Bias Electro Luminescence (ReBEL) studies were performed to localize Ni induced non-ohmic breakdown sites [7].

The adhesion of the plated contacts was tested with a ribbon soldered manually to the bus bar metal stack and ripped off under an angle of 90°. The measured peel force was recorded and normalized to a bus bar width of 1 mm.

Scanning electron microscope (SEM) studies of the contact profile and of the surface before and after peel tests were carried out to analyze the silicidation, defects and failing interfaces.

3 RESULTS AND DISCUSSION

The solar cells fabricated in this experiment were studied under two aspects, adhesion of the plated Ni-Cu contacts and electrical stability under the thermal stress applied for strong Ni silicidation. The following section will highlight the process effects on each aspect.

3.1 Contact adhesion effects

The results of the peel force measurement are summarized in Table 1 and the corresponding silicidation can be seen in profile in Figure 2

Table 1: Measured peel force under an angle of 90°

Group	*Median [N/mm]*	*Max [N/mm]*
1-HF	0	0.1
1-BHF [11]	0.5	1.3
2	1.2	1.7
3	0.8	1.5
4	0.2	0.4

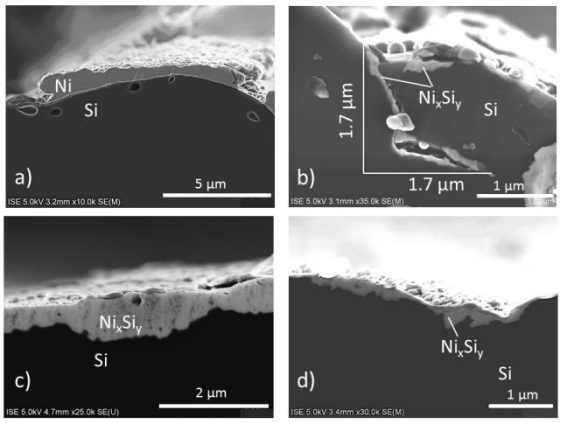

Figure 2: SEM cross section studies of silicidation behavior. a) Gr.1-HF - cw Laser Doping, b) Gr.2 - LCP Doping, c) Gr.3 -cw laser doping + Inkjet m&e, d) Gr.4 - cw laser doping + ns laser ablation. Note the different scaling of the pictures

Mondon et al. showed that Nickel silicide (Ni_xSi_y) formation improves the adhesion for plated Ni contacts [6]. Yet a diffusion barrier for plated Ni in form of SiO_2 and SiO_xN_y was already observed in combination with laser doping, which hinders the Ni_xSi_y formation and leads to a poor or no adhesion of the Ni-Cu contact[11, 12]. This can be seen in Table 1 especially in group 1 and 4. SEM measurements in Figure 2 a) and Figure 3 a) of solar cells of group 1 with simultaneous cw laser doping and SiN_x removal show almost no silicidation. Only minor Ni_xSi_y islands in the middle of the laser doped line are visible, (see Figure 3a). As expected a negligible peel force was measured. BHF treatment directly before Ni plating was performed to remove the oxides and more silicidation was observed in the laser doped area, (see Figure 3b). The peel forces improved to a mean peel force of 0.5 N/mm with BHF [11], similar to [12].

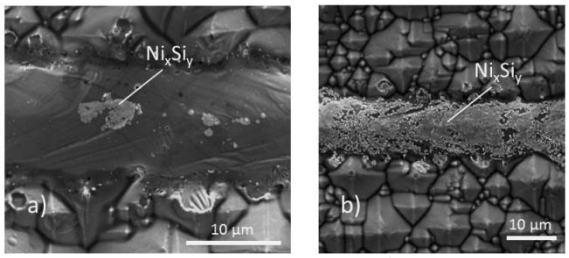

Figure 3: Top view SEM measurement of a cw laser doped line. a) group 1-HF pretreatment and b) group 1-BHF pretreatment after Ni plating and annealing [11]

More silicidation can be found in group 4, where the solar cells were cw laser doped before SiN_x deposition and a nanosecond laser removal of the SiN_x layer was performed. Yet the Ni_xSi_y layer formation follows the pulses, (see Figure 4). Formation of SiO_xN_y in a halo structure was observed in the outer pulse regions, which hinders the Ni diffusion and Ni_xSi_y formation. Temperature distribution of a single laser pulse with a duration of 80 ns matches the temperatures of SiN_x ablation in the center of the pulse and promoting SiO_xN_y formation in outer rims of the pulse [11]. Despite the silicidation, the peel tests showed still a poor adhesion with a maximum peel force of 0.4 N/mm. Failing

interface was observed to be between plated Ni-Cu contact and Ni_xSi_y. Although Ni_xSi_y has formed, the low peel force can be explained by the fact, that the contact area between Ni_xSi_y and Ni-Cu is still not high enough to form sufficient adhesion. Another failing interface was observed between Ni_xSi_y and Si itself. Chipping can be seen in Figure 4. Secondary laser induced defects in Si bulk through laser doping with a cw laser and dielectric structuring with a nanosecond laser weakens the material.

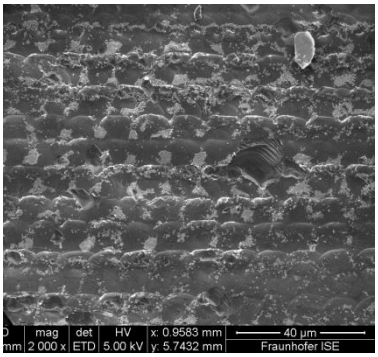

Figure 4: cw laser doped bus bar + ns SiN_x opening show Ni_xSi_y sites with halos around. Main failing interface is between Ni and Ni_xSi_y but also between Ni_xSi_y and Si due to chipping

LCP doped cells from group 2 show a quite high peel force of max 1.7 N/mm and a median of 1.2 N/mm. A high coverage Ni_xSi_y was observed. Yet chipping in the Si bulk is the dominant failure mechanism. Chipping along the LCP doped lines within a busbar after the peel test can be seen in Figure 5.

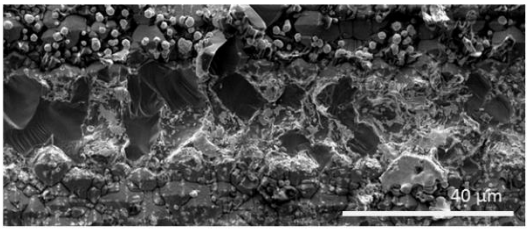

Figure 5: SEM top view of a single LCP doped line after peel test. Chipping along the line show the dominant failing procedure

The surface of the LCP structured area results in a non-planar topography, which on the one hand gives the possibility to anchor the plated contact in "micro cavities", (see Figure 2 b)). On the other hand a high density of micro cavities can lead to micro crack formation, which results in chipping in the peel test. These micro cavities may form from the melt and rapid recrystallization due to fluid cooling from the jet. A possible explenation is that the resulting forms can act as a lever in the peel test and enhance chipping.

A full faced Ni_xSi_y formation (see Figure 2 c)) and no chipping demonstrated the process sequence of group 3 with cw laser doping and an Inkjet M&E SiN_x opening. The peel forces were up to maximum of 1.5 N/mm and a median of 0.8 N/mm, which is comparable to the results from [11]. The failing interface is between the Ni and Ni_xSi_y.

3.2 Electrical effects

The electrical stability of the fabricated solar cells were characterized by measuring the *pFF* before plating and after plating and annealing. The results are summarized in Table 2.

Table 2: Pseudo fill factors of the presented groups before and after plating and annealing at a temperature of 450 °C for 10 min

Group	*pFF before plating and annealing [%]*	*pFF after plating and annealing [%]*
1-HF	84.5	81.4
1-BHF [11]	83.9	67.8
2	84.3	51.1
3	83.4	78.9
4	83.6	80.9

The nanosecond LCP doped solar cells showed Ni silicide formation, yet the silicidation has a negative effect on the electrical properties. It causes recombination active sites, which decreases the *pFF* of the solar cell, if silicides penetrate the space charge region [7]. Suns-V_{oc} measurement of the pseudo fill factor after plating and annealing showed significant decrease. Deep silicides of up to 1.7 µm can be found in micro cavities, which overshoot the middle pn junction depth of 1.2 µm and most likely spike through the space charge region. Figure 6 shows a ReBEL study of a LCP doped solar cell after plating and annealing. As demonstrated by [7, 8] the reverse bias breakdown sites visualized by ReBEL are for annealing-induced Ni shunts also the dominant recombination active sites under forward bias. The ReBEL images show recombination active breakdown sites within the laser doped area, especially in the bus bar region. This proves that the degradation is not a result of parasitic Ni plating within the passivated area, but can be corresponded to an improper selective emitter shape with a too shallow and inhomogeneous doping depth [8].

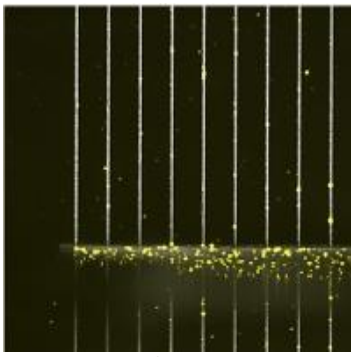

Figure 6: Superposition of a top view gray image (light structures are the plated metal contacts) of an LCP doped solar cell (group 2) after plating and annealing and a ReBEL measurement (yellow) spots visualize the recombination active breakdown sites.

Solar cells from group 1 with a simultaneous SiN_x passivation opening and cw laser doping have only small *pFF* degradation after plating and annealing, but as described in the previous section, the silicidation is very limited in the contact area. A BHF treatment showed an increase of Ni_xSi_y, but also a *pFF* decrease below 70 %. Reverse Bias Electro Luminescence (ReBEL) studies

proved that annealing induced Ni shunts are mostly located at the edge of the pyramid stumps at the edges of the laser lines where a very shallow pn junction depth is expected [11].

Solar cells of group 3 and 4 with cw laser doping proved stable *pFF* against annealing induced Ni shunts, since no silicides were found below the pn junction depth of 4.2 µm. The shallow doped regions at the boundaries of the laser doped regions were covered by SiN_x passivation layer, since the structuring of the passivation layer was done in one separate process step leaving a narrow contact opening. However both groups show minor *pFF* degradation. One reason for the degradation can be seen in the ReBEL measurement. Here the boundary areas of the bus bars show recombination active sites. Microscope studies of these areas showed laser induced micro cracks in which plated Ni can be found. During laser doping turnovers of the guided laser cause long dwell times on the substrate due to accelerations and causes tensions within the material. These tensions are most likely the origin of the crack formation, which induces cracks that are not passivated by the SiN_x layer. A shadow mask during laser processing can avoid these defects.

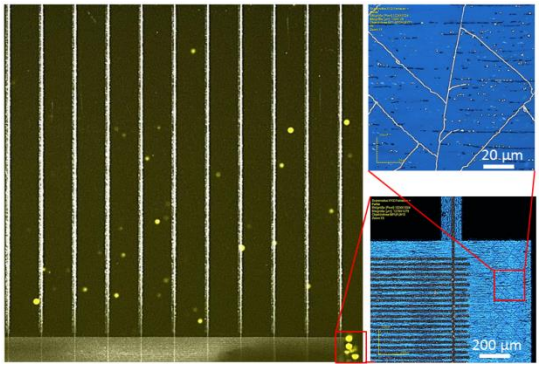

Figure 7: Left side: Superposition of a top view gray image (light structures are the plated metal contacts) of an cw laser doped solar cell (group 4) after plating and annealing and a ReBEL measurement (yellow). Two pictures on the right side show optical microscope pictures with parasitic Ni plating in the laser induced micro cracks.

4 CONCLUSION

This work presents the challenges of solar cells with plated metal based contacts combined with laser doped selective emitter design. The adhesion of the plated Ni contact is strongly influenced by the surface conditions of the laser doped Si. SiO_2 and SiO_xN_y interface layers were found after laser structuring of the SiN_x passivation with a cw laser. This interface layer hinders Ni_xSi_y formation resulting in poor contact adhesion. BHF treatment of the same process sequence improved the contact adhesion by removing the oxides, but decreasing the solar cell performance by Ni induced shunting in shallow doped boundary regions. Solar cells with LCP laser doped selective emitter structures show good contact adhesion, but no stability to Ni induced non-ohmic shunts due to shallow doping depth of about 1 µm.

Solar cells with plated Ni contacts and laser doped selective emitter can be obtained, if the silicide formation is not disturbed. The cell design has to guarantee that the pn junction is deeper than the Ni silicides throughout the contact area. This can be realized when the SiN_x removal is done separately from the doping step and the opening is narrower than the laser doped area.

REFERENCES

[1] S. R. Wenham, *et al.*, "Buried contact silicon solar cells," *Solar Energy Materials and Solar Cells*, vol. 34, pp. 101-10, 1994.

[2] Z. Shi, *et al.*, "Mass production of the innovative PLUTO solar cell technology," in *Proceedings of the 34th IEEE Photovoltaic Specialists Conference*, Philadelphia, Pennsylvania, USA, 2009, pp. 1922-6.

[3] T. M. Bruton, *et al.*, "Towards 20% efficient silicon solar cells manufactured at 60 MWp per annum," in *Proceedings of the 3rd World Conference on Photovoltaic Energy Conversion*, Osaka, Japan, 2003, pp. 899-902.

[4] *al.*, "Advanced PERC and PERL production cells with 20.3% record efficiency for standard commercial p-type silicon wafers," *PROGRESS IN PHOTOVOLTAICS: RESEARCH AND APPLICATIONS*, 2012.

[5] D. Kray, *et al.*, "Industrial LCP selective emitter solar cells with plated contacts," in *Proceedings of the 35th IEEE Photovoltaic Specialists Conference*, Honolulu, Hawaii USA, 2010, pp. 667-71.

[6] A. Mondon, *et al.*, "Microstructure analysis of the interface situation and adhesion of thermally formed nickel silicide for plated nickel–copper contacts on silicon solar cells," *Solar Energy Materials and Solar Cells*, vol. 117, 2013.

[7] A. Büchler, *et al.*, "Localization and characterization of annealing-induced shunts in Ni-plated monocrystalline silicon solar cells," *rrl solar*, 2014.

[8] S. Kluska, *et al.*, "Micro characterization of laser structured solar cells with plated Ni–Ag contacts," *Solar Energy Materials and Solar Cells*, vol. 120, 2014.

[9] A. Sugianto, *et al.*, "18.5% laser-doped solar cell on CZ p-type silicon," in *Proceedings of the 35th IEEE Photovoltaic Specialists Conference*, Honolulu, Hawaii USA, 2010, pp. 689-94.

[10] G. P. Willeke and D. Kray, "A new route towards 50 µm thin crystalline silicon wafer solar cells," in *Proceedings of the 17th European Photovoltaic Solar Energy Conference*, Munich, Germany, 2001, pp. 1621-4.

[11] C. Geisler, *et al.*, "Overcoming electrical and mechanical challenges of continuous wave laser processing for Ni--Cu plated solar cells," *Submitted to: Solar Energy Materials and Solar Cells*.

[12] C. Geisler, *et al.*, "Continuous wave laser processing for electrical and mechanical stable solar cells with Ni-Cu metallization," presented at the 4th International Conference on Silicon Photovoltaics, SiliconPV 2014, 2014.